Biointerface Research in Applied Chemistry
Platinum Open Access Journal (ISSN: 2069-5837)

Article
Volume 12, Issue 6, 2022, 7205 - 7213
https://doi.org/10.33263/BRIAC126.72057213

Surface Functionalized Halloysite with N-[3-(Trimethoxysilyl)Propyl] Ethylenediamine for Chromium and Nickel Adsorption from Aqueous Solution

Sulyani Fitri [1], Amri Yahya [1], Sheikh Ahmad Izaddin Sheikh Mohd Ghazali [2], Is Fatimah [1]

[1] Department of Chemistry, Faculty of Mathematics and Natural Sciences, Universitas Islam Indonesia, Kampus Terpadu UII, Jl. Kaliurang Km 14, Sleman, Yogyakarta, Indonesia; isfatimah@uii.ac.id (I.F.);
[2] Faculty of Applied Sciences, Universiti Teknologi MARA Cawangan Negeri Sembilan, Kampus Kuala Pilah, Kuala Pilah 72000, Negeri Sembilan, Malaysia;
* Correspondence: isfatimah@uii.ac.id (I.F.);

Scopus Author ID 35104706400

Received: 10.09.2021; Revised: 25.10.2021; Accepted: 29.10.2021; Published: 24.11.2021

Abstract: In this study, -[3-(trimethoxysilyl)propyl] ethylenediamine - modified Indonesian natural halloysite was applied for Cr(III) and Ni(II) adsorption from aqueous solution. The studies include the physicochemical characterization of the synthesized material by using XRD, SEM, gas sorption analyzer, and FTIR analyses. Furthermore, the adsorption experiments were performed at a batch system for investigating the adsorption kinetics and thermodynamic. The results showed no significant changes in either the material crystallinity or specific surface area, but the changes of surface functional groups identified the anchored ammine modifier. Kinetic modeling showed pseudo-second-order model best fitted the experimental data for both adsorbents. Moreover, the thermodynamic studies represented the chemisorption interaction of modified halloysite with the adsorbate since the average adsorption enthalpy values are at 44.3 kJ/mol and 41.70 kJ/mol for Cr(III) and Ni(II), respectively.

Keywords: adsorption; kaolinite; chromium; nickel.

1. Introduction

Considerable amounts of metals are used in many process industries, such as paint, ink, battery, and textile industries. The toxicity and fate of such metals, especially heavy metals, are the most concerned in industrial wastewater monitoring. Without proper treatment, the rest of the metal ions in aquatic and soil environments threats human health as they can easily be magnified and pre-concentrated by the food chain [1,2]. Due to these strong and serious reasons, the treatment of metal ions-containing wastewater needs to be optimized. Adsorption is the most popular method for uptake metal ions from the aquatic system due to its simplicity and ease in the operational scale. The development of high capacity and specificity of adsorbent is the most to get interested and attempted. Especially for heavy metals, including nickel and chromium, the searches of selective adsorbents with high capacity were recorded. In particular, to enhance the economic value of the adsorption process for many applications, the exploration of a low-cost adsorbent gets the most interest [3,4].

Previous research reported the special feature of functional natural minerals-based materials for some heavy metals. The applicability of the silica-alumina surface to be modified with a specific functional group having affinity to trap with metal ion is the main characteristic for adsorption capacity enhancement. Naturally occurring clay minerals offer

great potential because of their characteristic structure as the layered and three-dimensional formation [5,6]. The adjustable structure is the base for various technological applications based on the adsorptive and ionic. The use of natural minerals such as clay materials is valued to give economic value refer to the abundance source [3,7,8]. Within this topic, a previous paper has reported the functionalization of kaolinite with N-[3-(trimethoxysilyl)propyl] ethylenediamine, called APTES/Kaolinite for Pb(II) removal [9]. The anchored ammine functional group was significantly improving the adsorption capacity and reusability of Pb (II). However, there is no study on the removal of Cr(II) and Ni(II) by the material [10,11].

By a similar clay class such as kaolinite, halloysite is one of the typical minerals that have gotten more interest recently [12,13]. The feature of halloysite, such as its easy to be converted into many forms by surface functionalization, make it attractive for selective adsorption [12]. Refer to the big potency of halloysite mineral in Indonesia and as an exploration to contribute the data for heavy metal adsorption, this paper reports the modification of Indonesian halloysite with N-[3-(trimethoxysilyl)propyl] ethylenediamine [furthermore called as APTES/HAL] and the study for its capability in Cr(III) and Ni(II) adsorption from aqueous solution.

2. Materials and Methods

2.1. Materials.

Chemicals consisting of nickel chloride, chromium (III) nitrate, and N-[3-(trimethoxysilyl)propyl] ethylenediamine were purchased from Merck (Germany). Halloysite sample was obtained from the mining area of East Java, Indonesia, were washed with tap water to remove impurities, dried in an oven, ground, and sieved to a particle size range of 100 mesh.

2.2. Methods preparation of APTES/HAL.

The preparation of APTES/HAL from halloysite powder was conducted to refer to previous work. An APTES solution was slowly added to a halloysite suspension of 10 g of kaolinite in 100 mL of distilled water. Into the mixture, 0.2 M HCl was added and stirred for 4 h followed by refluxing for 6 h. The APTES content in the composite was set at 10 mmol/g. The solid from the reflux was obtained by drying suspension in an oven, and the result was encoded as APTES/HAL.

2.3. Characterization.

The character of APTES/HAL and HAL samples was analyzed using x-ray diffraction, gas sorption analyzer, Fourier Transform Infrared (FTIR) spectrometer, and SEM analysis. A Shimadzu X6000 XRD instrument was employed for the analysis, and a gas sorption analyzer, SEM-EDX of Phenom X, was employed at 0.2 μm resolution and a magnification of 10000×. Brunauer-Emmett-Teller (BET) measurements were performed on a NOVA 1200 quantachrom. The nitrogen adsorption isotherm values were determined at 77 K.

The adsorption experiments were conducted in a batch system using a horizontal shaker. For each adsorption experiment, 0.2 g of the adsorbent was added into a 250 mL solution. The amount of rest metal ions was determined using atomic absorption spectrophotometer (AAS). A Perkin-Elmer instrument was utilized.

2.4. Adsorption experiments.

The adsorption experiments were conducted in a batch system. For the study, varied contact time, adsorbents, and temperatures were applied. The adsorbed metal ion was calculated based on the metal ion concentration in the filtrate, which was measured by atomic absorption spectrophotometry. A Perkin-Elmer instrument was employed for the analysis.

3. Results and Discussion

3.1. Physicochemical character of the adsorbents.

Fig.1 shows the diffractograms of HAL and APTES/HAL. The presence of HAL is identified by the sharp reflection at 2θ of 20.1°which is the characteristic (1 1 0) halloysite together with the peaks at about 27.1° and 43.8° corresponding to (0 0 2) and (1 2 3) reflections, respectively [14]. Other peaks beside the halloysite representative are observed at around 30o, referred to as alunite, and at about 37° associated with the presence of kaolinite [15–17]. Both identified phases are usually found as the halloysite used here is the natural mineral. The APTES modification does not change the peaks presented, indicating that there was no chemical change during the process nor the physical influence.

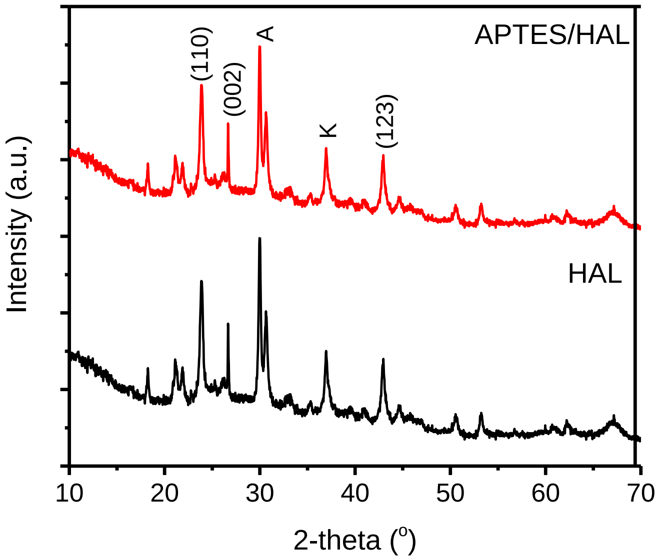

Figure 1. XRD pattern of HAL and APTES/HAL.

The FTIR spectra of HAL and APTES/HAL are presented in Fig.2.

Both solids show sharp and wide bands at the range of 3400-3690 $cm^{-1,}$ corresponding to the indication of O-H coming from water and hydroxyl-associated with Si-O and Al-O from halloysite structure. These bands are also associated with the absorption at around 1637-1641 $cm^{-1,}$ indicating the presence of a Si-OH group. The Si-O is also identified by the emergence of strong bands in the 462 cm^{-1} together with the presence of Si-O-Si with the absorption at 1044 cm^{-1} and 800 cm^{-1}. The attachment of APTES in APTES/HAL is identified with the vibration spectrum at 1384.12 cm^{-1} which indicates the vibration of primary N-H, and the vibration associated with C-H at around 2885.51 cm-1 coming from the propyl chain of

APTMS structure. Similar characteristics bands were also identified by such amine-modified silica surface and ammine-modified clay [9,18,19].

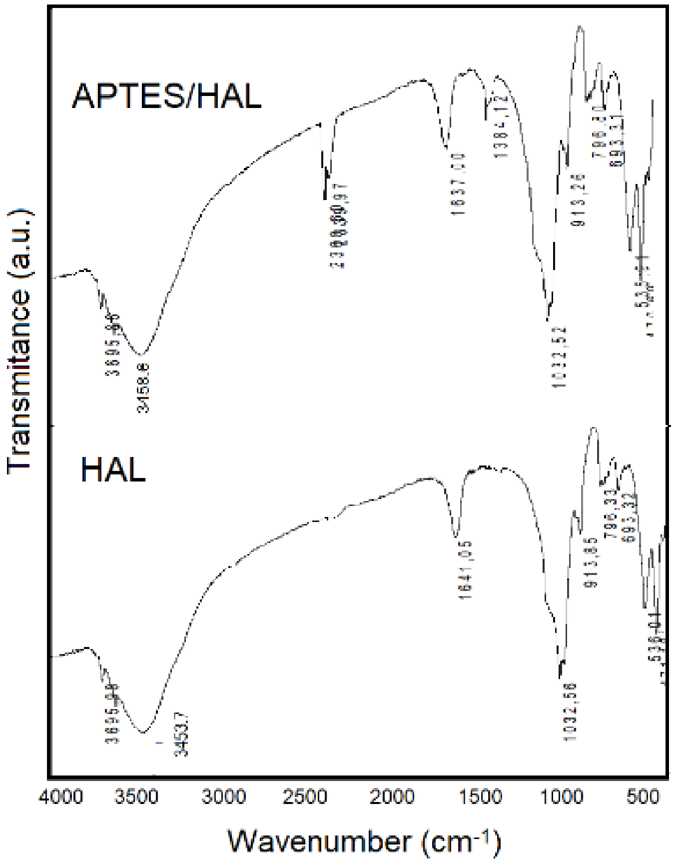

Figure 2. FTIR spectra of HAL and APTES/HAL.

The surface modification reflects the change of surface morphology as presented by SEM image in Fig.3. A relatively smoother surface is found in APTES/HAL; meanwhile, HAL represents the predefined characteristics morphology. From the EDX spectra, Si and Al are the main components of the materials with no significant change in amount. It was calculated that the Si/Al molar ratio of about 1.02 is found, which represents the halloysite and silica component in the natural mineral [20]. However, as the surface evolution was identified, the specific surface area of APTES/HAL is about 37.4 m^2/g which is not significantly different from HAL, which exhibits a specific surface area of about 39.7 m^2/g. A similar phenomenon was also reported in the APTES modification to kaolinite in that less surface area was found, but there is no such significant reduction [21].

The adsorption capability of the adsorbents was evaluated by measuring the adsorption capacity as a function of adsorption time, and the plot is presented in Fig.4.

From the plots, it can be seen that APTES/HAL gives a higher adsorption capacity compared to HAL at the time range of 30-120 min. The kinetics of the adsorption was evaluated refer to the pseudo-first-order, pseudo-second-order, and intra-particle diffusion kinetics by following equations (1-3):

$$\ln(q_e - q_t) = ln q_e - kt \qquad (1)$$

$$\frac{t}{q_t} = \frac{1}{k_2 q_e^2} + \frac{t}{q_e} \qquad (2)$$

$$q_t = k_i t^{0.5} + C \qquad (3)$$

where q_t (mg/g) is the amount of adsorbed metal ions at the time of t, q_e (mg/g) is adsorption capacity, k (min^{-1}) is the first-order rate constant, k_2 (g/mg min) is the second-order rate constant of adsorption (min^{-1}), k_i (mg.min$^{1/2}$/g) and C is constant are kinetics constant and the constant of the intra-particle diffusion model, respectively [22,23].

The calculated parameters listed in Table 1 exhibit that the adsorption data fit well with the pseudo-second-order kinetics.

The fitness of the pseudo-second-order kinetic model suggests that the Cr(III) and Ni(II) adsorption by both adsorbents is controlled by the chemisorption mechanism. Moreover, from the adsorption capacity values, the capacity enhancement is also found for both metal ions. The adsorption capacity for Cr by HAL is 30.37 mg/g increased into 41.88 mg/g by APTES/HAL. The enhancement also appears significantly for Ni, which is about 19.63 mg/g in HAL to be 34.08 mg/g by APTES/HAL. The kinetics order and the capacity values describe the presence of chemical interaction caused by the APTES anchored on the halloysite surface. The ammine functional group has an affinity to bind with the metal ions via coordination bonding [24,25]. According to Pearson's theory (Hard & Soft Acid-Base Theory), ammine functional groups are classified as intermediate ligands with high affinity towards transition metals, including Cr(III) and Ni(II). The electronegativity from the lone pair electrons of nitrogen and its weakly polarizable forced ammine functional group to bind with the small radii and weakly polarizable metal ions [26,27]. The schematic representation of the chemical interaction between metal ions and APTES is presented in Fig.5.

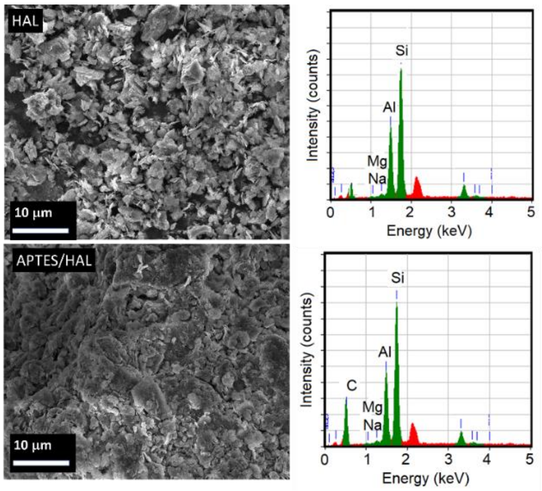

Figure 3. SEM-EDX analysis results of HAL and APTES/HAL.

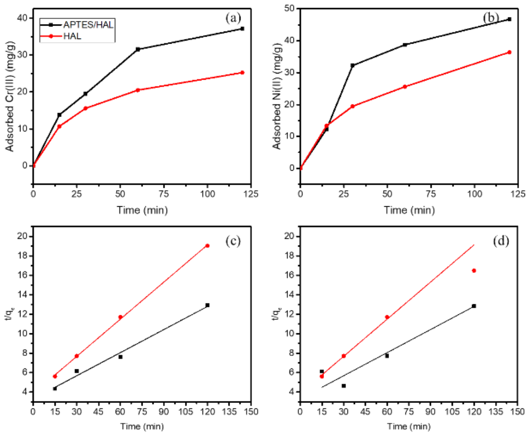

Figure 4. (a-b) Adsorption kinetics of Cr(III) and Ni(II) (c-d) pseudo-second-order plots of Cr(III) and Ni(II) adsorption.

Table 1. Calculated parameters from kinetics studies.

	Pseudo-first order kinetics					
	Cr (III)			**Ni(II)**		
	R^2	**k**	**Qe**	**R^2**	**k**	**Qe**
APTES/HAL	0.994	0.364	3.28	0.930	0.199	0.32
HAL	0.957	0.032	1.04	0.972	0.140	2.42
	Pseudo-second-order kinetics					
	Cr (III)			**Ni(II)**		
	R^2	**k**	**Qe**	**R^2**	**k**	**Qe**
APTES/HAL	0.998	41.88	12.64	0.999	1.22	34.08
HAL	0.994	30.37	7.86	0.990	0.77	19.63
	Intra-particle diffusion					
	R^2	**k_i**	**C**	**R^2**	**k_i**	**C**
APTES/HAL	0.989	0.0088	-0.033	0.969	0.001	0.79
HAL	0.989	0.419	-0.423	0.984	0.540	0.002

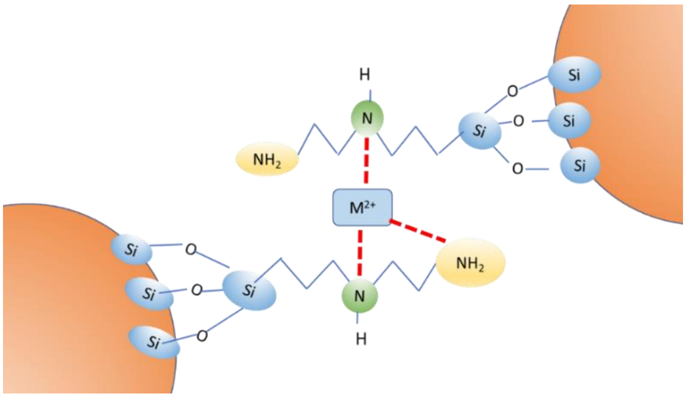

Figure 5. Schematic representation of adsorption interaction between APTES/HAL and metal ions.

3.2. Adsorption isotherm.

The detail of adsorbate-adsorbent interaction was evaluated by determining adsorption isotherm using two isotherm models; the Langmuir and Freundlich models. The equations for the Langmuir and Freundlich models are as follow (eq 4-5):

$$q_e = K_F C_e^{1/n} \qquad (4)$$

$$q_e = \frac{q_m K_L C_e}{1+K_L C_e} \qquad (5)$$

where q_e and q_m(mg/g) are the adsorption capacity of the adsorbent at the equilibrium and maximum value, Ce (mg/L) is the concentration of adsorbate in equilibrium, K_L (L/mg) is the Langmuir constant related to the energy of adsorption, and K_F *and n* are the Freundlich constants related with adsorption-desorption equilibrium, and adsorption intensity, respectively [28,29].

The R_L parameter from the Langmuir isotherm is represented as follows (eq. 6):

$$R_L = \frac{1}{1+K_L q_m} \qquad (6)$$

Table 2 lists the calculated isotherm parameters.

Table 2. Calculated isotherm parameters.

Metal ion	**Adsorbent**	**Freundlich Isotherm parameters**			**Langmuir Isotherm Parameters**			
		K_F (L/g)	**1/n**	**R^2**	**q_m (mg/g)**	**K_L (L/mg)**	**R_L**	**R^2**
Cr (III)	APTES/HAL	26.28	0.31	0.992	45.08	0.04	0.999	0.998
	HAL	1.78	0.57	0.998	26.23	1.28	1.050	0.928
Ni (II)	APTES/HAL	45.18	0.26	0.996	40.19	0.04	0.998	0.995
	HAL	7.85	0.48	0.954	42.13	1.93	0.995	0.854

The R^2 values represent that both models can be applied well for the Cr(III) and Ni(II) adsorption by APTES/HAL since the values are high (R^2~1). The Freundlich plots are presented in Fig.6. However, the HAL adsorbent shows the Freundlich isotherm's fitness rather than the Langmuir isotherm, as the R^2 value and the RL values are not appropriate to the model [30].

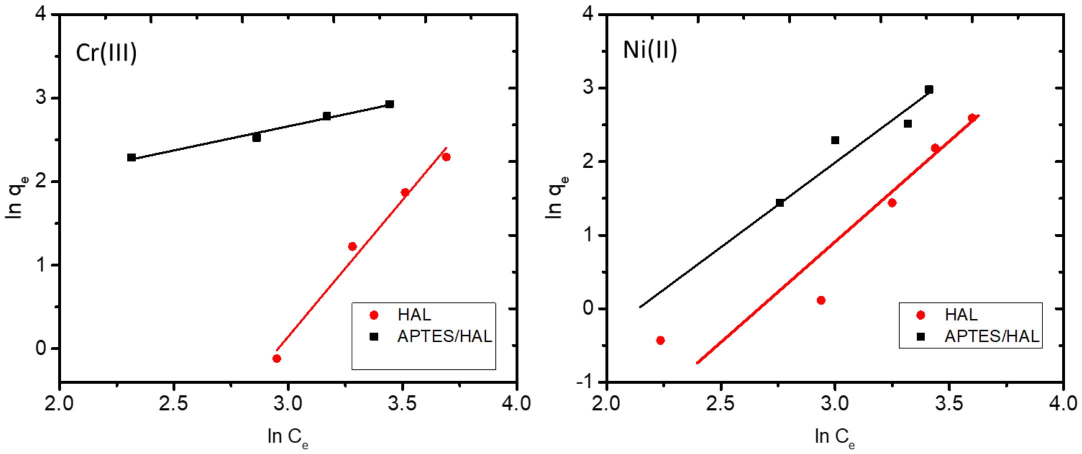

Figure 6. Freundlich isotherm plot of Cr(III) and Ni(II) adsorption.

Referring to RL values of the Langmuir isotherm model, the RL values laid at the range of 0< RL < 1 indicate the favorable adsorption, and the data represents the inappropriateness of Ni(II) adsorption by HAL. Moreover, all 1/n values from the Freundlich isotherm are less than 1, which validated the role of chemisorption on the adsorption sites. The KF values suggest that APTES/HAL demonstrates the higher adsorption/desorption equilibrium, meaning that the chemical equilibrium by APTES/HAL is more spontaneously occurred [10].

The isotherm data representing that the chemisorption interaction involved was confirmed by thermodynamic studies. The KF at varied temperatures were measured, and due to the adsorption standard free energy changes (ΔG^0) equation (4):

$$\Delta G^0 = RTlnK \qquad (4)$$

The average standard enthalpy change (ΔH^0) is presented as (eq.5) :

$$\ln K = -\frac{\Delta H^0}{R}\left(\frac{1}{T}\right) \qquad (5).$$

The average standard enthalpy values of Cr(III) and Ni(II) adsorption refer to the plot in Fig. 7, or called as vant' Hoff plot, is 44.3 kJ/mol and 41.70 kJ/mol, respectively. The values are matched with the chemisorption qualification in terms of heat of adsorption, which is laid in the range of 40-100 kJ/mol [25,31].

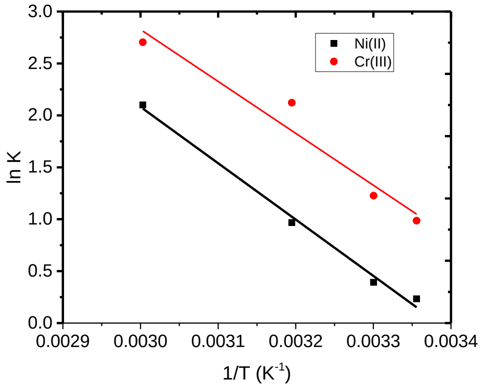

Figure 7. Van't Hoff plot of Cr(III) and Ni(II) adsorption by APTES/HAL.

4. Conclusions

Adsorption kinetics and thermodynamics of Cr(III) and Ni(II) by using -[3-(trimethoxysilyl)propyl] ethylenediamine -modified natural halloysite have been studied. The studies revealed the enhancement of adsorption capacity by surface modification with -[3-(trimethoxysilyl)propyl] ethylenediamine. The adsorption kinetics studies indicate that the adsorption reaction obeys pseudo-second-order reaction, and the thermodynamic studies demonstrate the chemisorption involved in the mechanism. Generally speaking, the data exhibit the promising application of modified natural halloysite an adsorbent for metal ions in wastewater treatment.

Funding

This research received no external funding.

Acknowledgments

The authors thank Chemistry Department, Universitas Islam Indonesia, for financial support to this research.

Conflicts of Interest

The authors declare no conflict of interest.

References

1. Soliman, N.K.; Moustafa, A.F. Industrial solid waste for heavy metals adsorption features and challenges; a review. *Journal of Materials Research and Technology* **2020**, *9*, 10235-10253, https://doi.org/10.1016/j.jmrt.2020.07.045.
2. Ayob, S.; Othman, N.; Altowayti, W.A.H.; Khalid, F.S.; Bakar, N.A.; Tahir, M.; Soedjono, E.S. A Review on Adsorption of Heavy Metals from Wood-Industrial Wastewater by Oil Palm Waste. *Journal of Ecological Engineering* **2021**, *22*, 249–265, https://doi.org/10.12911/22998993/132854.
3. Qiu, B.; Tao, X.; Wang, H.; Li, W.; Ding, X.; Chu, H. Biochar as a low-cost adsorbent for aqueous heavy metal removal: A review. *Journal of Analytical and Applied Pyrolysis* **2021**, *155*, https://doi.org/10.1016/j.jaap.2021.105081.
4. Puglla, E.P.; Guaya, D.; Tituana, C.; Osorio, F.; García-Ruiz, M.J. Biochar from Agricultural by-Products for the Removal of Lead and Cadmium from Drinking Water. *Water* **2020**, *12*, https://doi.org/10.3390/w12102933.
5. Yang, J.; Huang, B.; Lin, M. Adsorption of Hexavalent Chromium from Aqueous Solution by a Chitosan/Bentonite Composite: Isotherm, Kinetics, and Thermodynamics Studies. *Journal of Chemical & Engineering Data* **2020**, *65*, 2751-2763, https://doi.org/10.1021/acs.jced.0c00085.
6. Malovanyy, M.; Palamarchuk, O.; Trach, I.; Petruk, H.; Sakalova, H.; Soloviy, K.; Vasylinych, T.; Tymchuk, I.; Vronska, N. Adsorption Extraction of Chromium Ions (III) with the Help of Bentonite Clays. *Journal of Ecological Engineering* **2020**, *21*, 178-185, https://doi.org/10.12911/22998993/125545.
7. Hussain, S.T.; Ali, S.A.K. Removal of Heavy Metal by Ion Exchange Using Bentonite Clay. *Journal of Ecological Engineering* **2021**, *22*, 104-111, https://doi.org/10.12911/22998993/128865.
8. Chai, J.-B.; Au, P.-I.; Mubarak, N.M.; Khalid, M.; Ng, W.P.-Q.; Jagadish, P.; Walvekar, R.; Abdullah, E.C. Adsorption of heavy metal from industrial wastewater onto low-cost Malaysian kaolin clay–based adsorbent. *Environmental Science and Pollution Research* **2020**, *27*, 13949-13962, https://doi.org/10.1007/s11356-020-07755-y.
9. Fatimah, I. Preparation, characterization and physicochemical study of 3-amino propyl trimethoxy silane-modified kaolinite for Pb(II) adsorption. *Journal of King Saud University - Science* **2018**, *30*, 250-257, https://doi.org/10.1016/j.jksus.2017.04.006.
10. Mao, S.; Gao, M. Functional organoclays for removal of heavy metal ions from water: A review. *Journal of Molecular Liquids* **2021**, *334*, https://doi.org/10.1016/j.molliq.2021.116143.

11. Muhammad, A.; Shah, A.U.; Bilal, S. Effective Adsorption of Hexavalent Chromium and Divalent Nickel Ions from Water through Polyaniline, Iron Oxide, and Their Composites. *Applied Sciences* **2020**, *10*, https://doi.org/10.3390/app10082882.
12. Gray-Wannell, N.; Holliman, P.J.; Greenwell, H.C.; Delbos, E.; Hillier, S. Adsorption of phosphate by halloysite (7 Å) nanotubes (HNTs). *Clay Minerals* **2020**, *55*, 184-193, https://doi.org/10.1180/clm.2020.24.
13. Jabłońska, B. Optimization of Ni(II), Pb(II), and Zn(II) Ion Adsorption Conditions on Pliocene Clays from Post-Mining Waste. *Minerals* **2021**, *11*, 568–579, https://doi.org/10.3390/min11060568.
14. Lim, S.; Park, S.; Sohn, D. Modification Of Halloysite Nanotubes For Enhancement Of Gas-Adsorption Capacity. *Clays and Clay Minerals* **2020**, *68*, 189-196, https://doi.org/10.1007/s42860-019-00059-4.
15. Kuśmierek, K.; Świątkowski, A.; Wierzbicka, E.; Legocka, I. Enhanced adsorption of Direct Orange 26 dye in aqueous solutions by modified halloysite. *Physicochem. Probl. Miner. Process.* **2020**, *56*, 693-701, https://doi.org/10.37190/ppmp/124544.
16. Gray-Wannell, N.; Holliman, P.J.; Greenwell, H.C.; Delbos, E.; Hillier, S. Adsorption of phosphate by halloysite (7 Å) nanotubes (HNTs). *Clay Minerals* **2020**, *55*, 184-193, https://doi.org/10.1180/clm.2020.24.
17. Falcón, J.M.; Sawczen, T.; Aoki, I.V. Dodecylamine-Loaded Halloysite Nanocontainers for Active Anticorrosion Coatings. *Frontiers in Materials* **2015**, *2*, 1-3, https://doi.org/10.3389/fmats.2015.00069.
18. Barman, M.; Mahmood, S.; Augustine, R.; Hasan, A.; Thomas, S.; Ghosal, K. Natural halloysite nanotubes /chitosan based bio-nanocomposite for delivering norfloxacin, an anti-microbial agent in sustained release manner. *International Journal of Biological Macromolecules* **2020**, *162*, 1849-1861, https://doi.org/10.1016/j.ijbiomac.2020.08.060.
19. Jang, E.-H.; Pack, S.P.; Kim, I.; Chung, S. A systematic study of hexavalent chromium adsorption and removal from aqueous environments using chemically functionalized amorphous and mesoporous silica nanoparticles. *Scientific Reports* **2020**, *10*, 1–20, https://doi.org/10.1038/s41598-020-61505-1.
20. Zhu, X.; Fan, X.; Wang, Y.; Zhai, Q.; Hu, M.; Li, S.; Jiang, Y. Amino modified magnetic halloysite nanotube supporting chloroperoxidase immobilization: enhanced stability, reusability, and efficient degradation of pesticide residue in wastewater. *Bioprocess and Biosystems Engineering* **2021**, *44*, 483-493, https://doi.org/10.1007/s00449-020-02458-7.
21. Jeamjumnunja, K.; Cheycharoen, O.; Phongzitthiganna, N.; Hannongbua, S.; Prasittichai, C. Surface-Modified Halloysite Nanotubes as Electrochemical CO2 Sensors. *ACS Applied Nano Materials* **2021**, *4*, 3686-3695, https://doi.org/10.1021/acsanm.1c00174.
22. Zou, C.; Liang, J.; Jiang, W.; Guan, Y.; Zhang, Y. Adsorption behavior of magnetic bentonite for removing Hg(ii) from aqueous solutions. *RSC Advances* **2018**, *8*, 27587-27595, https://doi.org/10.1039/c8ra05247f.
23. Lee, W.; Yoon, S.; Choe, J.K.; Lee, M.; Choi, Y. Anionic surfactant modification of activated carbon for enhancing adsorption of ammonium ion from aqueous solution. *Science of The Total Environment* **2018**, *639*, 1432-1439, https://doi.org/10.1016/j.scitotenv.2018.05.250.
24. Cheah, W.-K.; Sim, Y.-L.; Yeoh, F.-Y. Amine-functionalized mesoporous silica for urea adsorption. *Materials Chemistry and Physics* **2016**, *175*, 151-157, https://doi.org/10.1016/j.matchemphys.2016.03.007.
25. Yokoi, T.; Kubota, Y.; Tatsumi, T. Amino-functionalized mesoporous silica as base catalyst and adsorbent. *Applied Catalysis A: General* **2012**, *421-422*, 14-37, https://doi.org/10.1016/j.apcata.2012.02.004.
26. Alfarra, A.; Frackowiak, E.; Béguin, F. The HSAB concept as a means to interpret the adsorption of metal ions onto activated carbons. *Applied Surface Science* **2004**, *228*, 84-92, https://doi.org/10.1016/j.apsusc.2003.12.033.
27. Astier, C.; Chaleix, V.; Faugeron, C.; Ropartz, D.; Krausz, P.; Gloaguen, V. Biosorption of lead (II) on modified barks explained by the hard and soft acids and bases (HSAB) theory. *Bioresources* **2012**, *7*, 1100-1110.
28. Dada A.O.; Olalekan A.P.; Olatunya A.M.; Dada O. Langmuir, Freundlich, Temkin and Dubinin–Radushkevich Isotherms Studies of Equilibrium Sorption of Zn 2+ Unto Phosphoric Acid Modified Rice Husk. *IOSR J. Appl. Chem.* **2012**, *3*, 38–45, https://doi.org/10.9790/5736-0313845.
29. Khezrianjoo, S.; Revanasiddappa, H. Langmuir-Hinshelwood Kinetic Expression for the Photocatalytic Degradation of Metanil Yellow Aqueous Solutions by ZnO Catalyst. *Chem. Sci. J.* **2012,** *2012*, 85–85.
30. Camara L.D.T.; Neto A.J. Modeling of the Kinetics of Salycilic Acid Adsorption in Polymeric and Activated Charcoal Adsorbents. *Ciencia* **2008,** *7*, 49–54, http://dx.doi.org/10.5380/reterm.v7i1.61741.
31. Alasadi, A.M.; Khaili, F.I.; Awwad, A.M. Adsorption of Cu (II), Ni (II) and Zn (II) ions by nano kaolinite : Thermodynamics and kinetics studies. *Chem. Inter.* **2020**, *5*, 258-268, https://doi.org/10.5281/zenodo.2644985.